



"HENRI COANDA"
AIR FORCE ACADEMY
ROMANIA



"GENERAL M.R. STEFANIK"
ARMED FORCES ACADEMY
SLOVAK REPUBLIC

INTERNATIONAL CONFERENCE of SCIENTIFIC PAPER AFASES
Brasov

ANALYSIS OF ROBUSTNESS OF THE UAV STABILITY AUGMENTATION SYSTEMS

Róbert SZABOLCSI*

*Faculty of Mechanical and Safety Engineering 'Bánki Donát', Óbuda University, Budapest, Hungary

Abstract: *This paper deals with analysis of the robust analysis of the UAV longitudinal motion stability augmentation system (SAS). In classical interpretation of the automatic flight control system's theory the aircraft or the UAV is considered as the rigid-body one. The controller stabilizing automatically UAV spatial motion is designed for the nominal plant. In real flight conditions UAV behaves elastically. The most common mathematical representation of the aircraft fuselage bending motion is the transfer function method. Mathematical model of the elastic UAV motion can be considered as additive uncertainty. The purpose of the authors is to analyze if the given static controller able to stabilize the UAV spatial motion when its real dynamics is taken into account during controller gain selection.*

Keywords: *elastic motion dynamics, additive uncertainty, robustness, SAS, additive stability margin.*

1. INTRODUCTION

This paper is lean upon early work of the author dealing with analysis of the robustness of the automatic control systems in general [1], and on paper representing application of this theory to analyze stability augmentation system of the UAV [2].

The true control systems are highly nonlinear with complicated dynamics. The controller of the closed loop systems is often designed using simplified mathematical model of the plant. Simplification means linearization of the nonlinear systems, pole zero cancellation etc. Elements of the control systems are often considered to be linear with simple mathematical models.

Neglecting nonlinearities, simplification of the dynamics of actuators, motors, sensors and amplifiers leads to the so-called nominal systems. However, controller must work with the true system in real environment.

Knowledge of the UAV elastic motion is important for designers from the point of view of derivation of the sensor location on the UAV. If elastic motion results in the error of

rate sensing it is necessary to filter electric signals of the sensors.

Many UAV, or aircraft flight control system is equipped with butterworth filters designed for filtering unwanted signals from the first and second overtones [4, 6, 7, 8]. The question is how to model the elastic motion of the UAV, or aircraft? One of the possible methods is the classical representation based upon the transfer function method.

This paper deals with representation of the high frequency elastic motion dynamics of the UAV using transfer function method.

Theoretical backgrounds, main methods of dealing with and equations of the aeroelasticity are given in [1, 4, 5, 6, 7, 11]. There are two methods available for modeling UAV, or aircraft elastic motion, i.e. classical and modern methods.

This paper applies classical method based on transfer functions. In [5, 6, 7, 12, 13, 14, 15, 16] there are given block diagrams of the automatic flight control systems, which are based upon stability augmentation systems.

Flying qualities of the automatic flight control systems are defined in [7, 8, 10, 13].

Analysis of the control system robustness is presented in [9, 17].

References [12, 14, 17] give some examples of the robust dynamic controller and filter design for the aeroelastic fighter automatic flight control system using both LQG and LQG/LTR design methods.

In [19] Palik deals with UAV flight management and flight safety aspects of the UAV flights. Palik and Vas dealt with UAV applications in aerodromes, and with its legal and airspace management aspects [20].

There are many UAVs owning non-conventional fuselage and wing design. The Helios UAV is a solar-powered HALE¹ UAV, propelled with electrical engines (see I.1.)



I.1. Helios Solar HALE UAV (www.google.com)

The Helios UAV does not have wing or fuselage in the classical meaning.

The strategic reconnaissance UAV ‘AeroVironment’ is the non-conventional UAV with large wingspan. The UAV fuselage is not a conventional one, i.e. it is very close to that of the long, thin rod (see I.2.a., I.2.b.)



I.2.a. AeroVironment HALE UAV (www.google.com).



I.2.b. AeroVironment HALE UAV (www.google.com).

The scientific research of the UAV in India resulted in DRDO HALE UAV (see I.3.)



I.3. Indian DRDO HALE UAV (www.google.com).

Next example of the non-conventional design of the HALE UAV is the Zephyr HALE UAV.



I.4. Zephyr HALE Solar UAV (www.google.com).

It is easy to see that new aerodynamic design and new materials applied in manufacturing of the modern UAVs results in a highly aeroelastic aircraft.

2. MATHEMATICAL MODEL OF THE ELASTIC UAV, AND ELASTIC AIRCRAFT

During mathematical modeling of the elastic UAV the fuselage and the wings elastic motion can be analyzed. The UAV fuselage is

¹ High Altitude Long Endurance



"HENRI COANDA"
AIR FORCE ACADEMY
ROMANIA



"GENERAL M.R. STEFANIK"
ARMED FORCES ACADEMY
SLOVAK REPUBLIC

INTERNATIONAL CONFERENCE of SCIENTIFIC PAPER AFASES
Brasov

considered as a simple rod and its bending distortion can be analyzed using Fig 1.

The slender beam differential equation of the vertical displacement w of any fuselage segment when pure bending deflection of this element is considered is given by [2, 3, 4, 5]:

$$\frac{\partial^2}{\partial x^2} \left[EI \frac{\partial^2 W(x,t)}{\partial x^2} \right] + m(x) \frac{d^2 [W(x,t)]}{dt^2} = F_y(x,t) \quad (2.1)$$

In eq (2.1) EI is bending stiffness, $m(x)$ is running mass, the mass per unit of the fuselage distance, $W(x,t)$ is the vertical displacement of the elements of the fuselage and finally, $F_y(x,t)$ is the running external load.

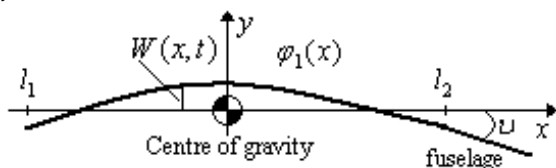


Fig 1. UAV fuselage bending motion
 v – angular deflection related to the fuselage unstrained position

Displacement $W(x,t)$ of any fuselage segment from its unstrained initial position can be derived as

$$W(x,t) = \sum_{i=1}^{\infty} \varphi_i(x) q_i(t), \quad (2.2)$$

where: $\varphi_i(x)$ – i th normal mode shape function, $q_i(t)$ – i th mode generalized coordinate. Substituting eq(2.2) into eq(2.1) and applying the property of the normal modes, which states that

$$\sum_{i=1}^{\infty} \omega_i^2 = \frac{\frac{\partial^2}{\partial x^2} \left[EI \frac{\partial^2 \varphi_i(x)}{\partial x^2} \right]}{m(x) \sum_{i=1}^{\infty} \varphi_i(x)}, \quad (2.3)$$

leads to the following equation:

$$m(x) \sum_{i=1}^{\infty} \varphi_i(x) \frac{d^2 q_i(t)}{dt^2} +$$

$$+ m(x) \sum_{i=1}^{\infty} \left(\varphi_i(x) \omega_i^2 q_i(t) \right) = F_y(x,t) \quad (2.4)$$

or, in the other manner:

$$\sum_{i=1}^{\infty} \left[\varphi_i(x) \frac{d^2 q_i(t)}{dt^2} + \varphi_i(x) \omega_i^2 q_i(t) \right] m(x) = F_y(x,t) \quad (2.5)$$

The distributed external load $F_y(x,t)$ at station x_E can be expressed as follows:

$$F_y(x,t) = F_y(t) \delta(x - x_E) \quad (2.6)$$

In the case when the external load $F_y(x,t)$ is developed by the angular deflection of the elevator – mounted at station with coordinate of x_E – the distributed load can be determined as:

$$F_y(x,t) = K_E \delta_E(t) \delta(x - x_E), \quad (2.7)$$

where: $\delta_E(t)$ – angular deflection of elevator, and, K_E – elevator gain. Applying Lagrange technique for the determination of the fuselage bending motion we have [2, 3, 4, 5, 6, 12, 17]:

$$M_i (\ddot{q}_i + 2\xi_i \omega_i \dot{q}_i + q_i \omega_i^2) = F_i(t), \quad (2.8)$$

where $M_i = \int_{-l_1}^{l_2} m(x) \varphi_i^2(x) dx$ – generalized mass of the i th elastic mode,

$F_i(t) = \int_{-l_1}^{l_2} \varphi_i(x) F_y(x,t) dx$ – generalized force of the i th elastic degree of freedom.

Substituting eq. (2.7) into equation of $F_i(t)$ defined above leads to:

$$F_i(t) = K_E \varphi_i(x) \Big|_{x=x_E} \delta_E(t) \quad (2.9)$$

The fuselage bending motion equation (2.8) respecting eq. (2.9) can be rewritten in the following manner:

$$\frac{d^2 q_i(t)}{dt^2} + 2\xi_i \omega_i \frac{dq_i}{dt} + \omega_i^2 q_i(t) = K_1 \delta_E(t) \quad (2.10)$$

where: $K_1 = \frac{K_E}{M_i} \varphi_i(x) \Big|_{x=x_E}$ – constant gain.

When the aeroelastic bending modes of the fuselage are taken into account to determine the output signal of the pitch rate sensor, in the complex frequency domain we have:

$$\omega_{z_E}(s) = s\nu(s) = \sum_{i=1}^{\infty} s q_i(s) \left(\frac{d\varphi_i(x)}{dx} \right) \Big|_{x=x_S} \quad (2.11)$$

where: $\omega_{z_E}(s)$ – pitch rate of the elastic UAV.

Secondly, taking the Laplace transform of eq. (2.10) with zero initial conditions we have:

$$(s^2 + 2\xi_i \omega_i s + \omega_i^2) q_i(s) = K_1 \delta_E(s). \quad (2.12)$$

It is easily can be seen that output signal of the pitch rate sensor can be determined as follows:

$$\omega_{z_E}(s) = \sum_{i=1}^{\infty} \frac{s K_i}{s^2 + 2\xi_i \omega_i s + \omega_i^2} \delta_E(s), \quad (2.13)$$

where $K_i = \frac{K_E}{M_i} \varphi_i(x) \left(\frac{d\varphi_i(x)}{dx} \right) \Big|_{x=x_E}$ is the gain

of the i th elastic degree of freedom.

In [5, 6, 12, 17] parameters of the 1st and the 2nd overtones of the high maneuverability UAV/aircraft fuselage elastic bending motion are given as follows:

$$\begin{aligned} K_1 &= 10 s^{-2}, \omega_1 = 10 s^{-1}, \xi_1 = 0,05 \\ K_2 &= 5 s^{-2}, \omega_2 = 20 s^{-1}, \xi_2 = 0,02 \end{aligned} \quad (2.14)$$

It is supposed that the longitudinal motion control system is affecting only the short period motion. The simplified mathematical model of the longitudinal motion of the rigid aircraft for the flight conditions $H=1000$ m and $M=0.4$ is given in [5, 6, 7, 12, 14, 15, 17] as follows:

$$\omega_{z_R}(s) = - \frac{A(1+sT)\omega_\alpha^2}{s^2 + 2s\xi_\alpha\omega_\alpha + \omega_\alpha^2} \delta_E(s). \quad (2.15)$$

In eq(2.15) let us consider the following parameters of the aircraft [5, 6, 12, 17]:

$$A=1,5 s^{-1}; T_\theta = 2 s; \omega_\alpha = 5 s^{-1}; \xi_\alpha = 0,5. \quad (2.16)$$

The resulting output signal of the pitch rate gyro can be determined as sum of the rigid and elastic aircraft output signals defined by eqs (2.13) and (2.15):

$$\omega_z(s) = \omega_{z_E}(s) + \omega_{z_R}(s) \quad (2.17)$$

The aeroelastic aircraft model built by eqs (2.13), (2.15) and (2.17) is represented in Fig 2.

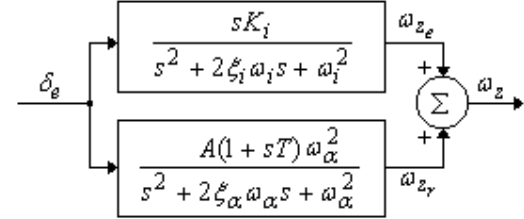


Fig 2. The rigid UAV longitudinal motion model perturbed by elastic high frequency model dynamics.

Sign ‘-‘ in rigid aircraft transfer function is for direction measuring between elevator deflection and the pitch rate. Elevator deflection is supposed to be positive if leads to negative pitch rate. If to neglect this sign in pitch rate damper the feedback must be positive.

3. TIME DOMAIN ANALYSIS OF THE LONGITUDINAL STABILITY AUGMENTATION SYSTEM

Let us consider the aircraft model defined by eqs(2.15)–(2.16). Eigenvalues and dynamic performances of the uncontrolled rigid aircraft are as follows [16, 18]:

$$\lambda_{1,2} = -2,5 \pm 4,33i, \xi = 0,5, \omega = 5 rad / s \quad (3.1)$$

Dynamic performances of the uncontrolled aircraft are different from the desired ones e.g in general case damping ratio must lie between 0,6 and 0,8 [7, 8, 10, 13].

Assuming high natural frequency of the rate gyro it can be modeled as a simple proportional term with static gain of $K_s = 1,5$. The compensator is supposed to be proportional term of $K_c = 2$.

During analysis of the pitch rate it is supposed that hydraulic actuator of the damper has fast response to input signals without any



"HENRI COANDA"
AIR FORCE ACADEMY
ROMANIA



"GENERAL M.R. STEFANIK"
ARMED FORCES ACADEMY
SLOVAK REPUBLIC

INTERNATIONAL CONFERENCE of SCIENTIFIC PAPER AFASES
Brasov

time delay. Simplified block diagram of the longitudinal stability augmentation system of the aircraft when its elastic motion is taken into account can be seen in Fig 3.

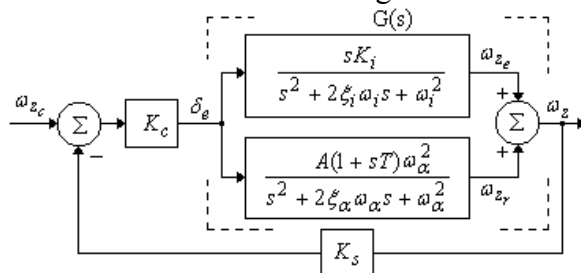


Fig 3. Longitudinal Motion Stability Augmentation System.

The uncontrolled and the controlled aircraft was analyzed in the time domain. Results of the computer simulation can be seen in Fig 4. From Fig 4. it is easily can be seen that the uncontrolled aircraft transient response has large overshoot and large response time.

The controlled rigid aircraft has faster response without overshoot. Dynamic performances of the closed loop system are as follows [2, 16, 18]:

$$\begin{aligned} \lambda_1 &= -0,599, \lambda_2 = -229 \\ \xi_1 &= \xi_2 = 1 \\ \omega_1 &= 0,599rad/s, \omega_2 = 229rad/s \end{aligned} \quad (3.2)$$

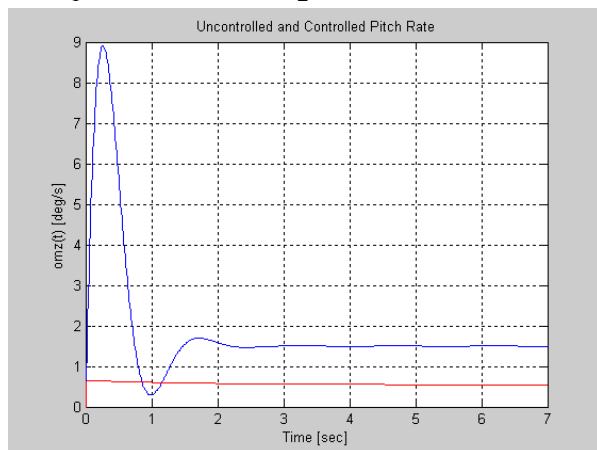


Fig 4. Aircraft pitch rate step responses.
uncontrolled rigid aircraft controlled rigid aircraft

The closed loop perturbed control system was analyzed in the time domain. Results of the computer simulation can be seen in Fig 5.

From Fig 5. it is easily can be seen that first and the second elastic motion overtones lead to slight oscillation caused by dynamics of the first overtone.

Dynamic performances of the closed loop control flight control system were found using [2, 16, 18] to be:

$$\begin{aligned} \lambda_{1,2} &= -0,519 \pm 1,95i; \xi_{1,2} = 0,0266; \omega_{1,2} = 1,95rad/s \\ \lambda_3 &= -0,58; \xi_3 = 1; \omega_3 = 0,58rad/s \\ \lambda_{4,5} &= -0,729 \pm 9,52i; \xi_{4,5} = 0,0764; \omega_{4,5} = 9,54rad/s \\ \lambda_6 &= -274; \xi_6 = 1; \omega_6 = 274rad/s \end{aligned} \quad (3.3)$$

From eq. (3.3) follows that complex conjugate roots of $\lambda_{1,2}$, and, $\lambda_{4,5}$ are developed by the elastic motion high frequency dynamics.

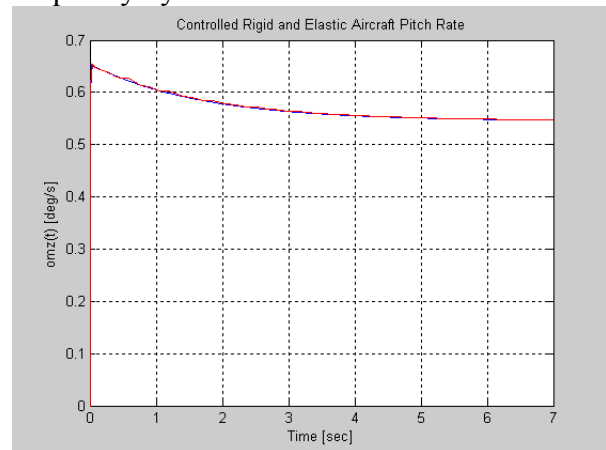


Fig 5. Aircraft pitch rate responses.
controlled rigid aircraft controlled elastic aircraft

4. FREQUENCY DOMAIN ANALYSIS OF THE LONGITUDINAL STABILITY AUGMENTATION SYSTEM OF THE AIRCRAFT

Robust stability analysis gives answer to question 'if the static controller is able to stabilize the true plant?' Firstly, let us analyze

the frequency domain behavior of the additive uncertainty. Bode diagram of the uncertainty can be seen in Fig 6.

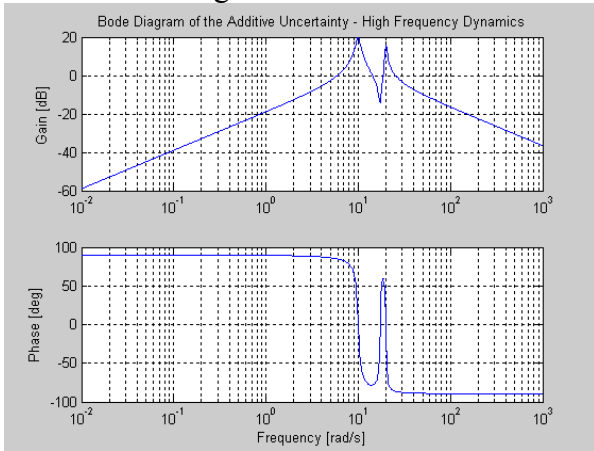


Fig 6. Bode diagram of the additive uncertainty.

Uncertainty gain has resonance peak at 5 rad/s. This is because of the D-term in the numerator of eq. (2.13). Both in low and in high frequency domain the gain is small. The additive uncertainty affects the open loop system frequency domain behavior. Results of the computer simulation can be seen in Fig 7.

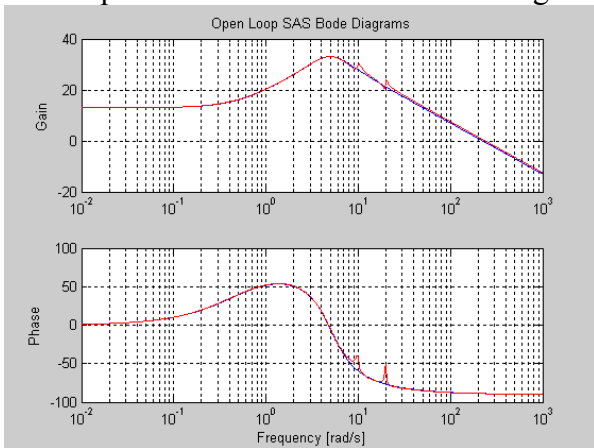


Fig 7. Bode Diagram of the Open Loop Nominal and Perturbed Systems.
nominal SAS perturbed SAS

From Fig 7. it can be seen the effect from elastic motion dynamics, which can be considered for additive uncertainty. At resonance frequencies of 5 rad/s and at 10 rad/s the gain and the phase angle have peak in their values. The open loop gain and the phase angle are increased only at the resonance frequency and in its bordering domain.

5. ROBUSTNESS ANALYSIS OF THE LONGITUDINAL STABILITY AUGMENTATION SYSTEM OF THE AIRCRAFT

From Fig 3. following transfer functions can be obtained [1, 2, 7]:

$$S(s) = \frac{1}{1 + K_c(s)K_s(s)G(s)}, \quad (5.1)$$

which is sensitivity transfer function, and,

$$T(s) = \frac{K_c(s)G(s)}{1 + K_s(s)K_c(s)G(s)}, \quad (5.2)$$

which is closed loop complementary transfer function.

Using simplified block diagram of SAS (see Fig 3.), and using eq (2.16), and parameters defined for sensor transfer function, and the feedforward static controller, sensitivity and complementary transfer functions were found to be [16, 18]:

$$T(s) = \frac{150s + 75}{s^2 + 230s + 137,5}, \quad (5.3)$$

$$S(s) = \frac{s^2 + 5s + 25}{s^2 + 230s + 137,5}. \quad (5.4)$$

Results of the computer simulation in the frequency domain can be seen in Fig 8.

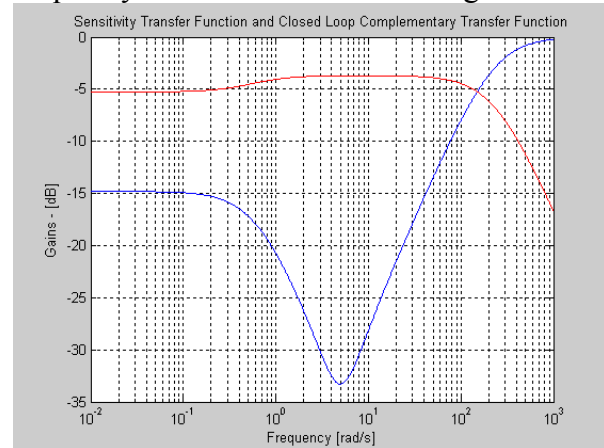


Fig 8. Sensitivity and the Closed Loop Complementary Transfer Functions.
Closed loop complementary transfer function of T(s)
Sensitivity transfer function of S(s)

Conditions of robust stability under additive uncertainty can be determined using the small-gain theorem.

INTERNATIONAL CONFERENCE of SCIENTIFIC PAPER AFASES
Brasov

Transfer function seen by the additive uncertainty is given by

$$M_a(s) = \frac{-K_s K_c}{1 + K_s K_c G(s)} \quad (5.5)$$

The feedback system will be robustly stable if takes place the following inequality:

$$|\Delta_a(s)| < \frac{1}{|K_s K_c [1 + K_s K_c G(s)]^{-1}|} \quad (5.6)$$

or in other manner

$$|\Delta_a(s)| < \frac{1}{|K_s K_c S(s)|} \quad (5.7)$$

From eq (5.6) it is evident that the closed loop system equipped with static controller can be said robustly stable if and only if additive uncertainty gain $|\Delta_a(s)|$ less than magnitude of the inverse of transfer function of $M_a(s)$.

If the additive uncertainty is stable and bounded one can write that

$$|\Delta_a(s)| < \frac{1}{\gamma} \quad (5.8)$$

The closed loop robust stability can be guaranteed if

$$|K_s K_c S(s)| < \frac{1}{\gamma}, \text{ or } |\gamma K_s K_c S(s)| < 1. \quad (5.9)$$

The *Additive Stability Margin (ASM)* can be defined by

$$ASM = \frac{1}{\sup_{\omega} |K_s K_c S(j\omega)|} \quad (5.10)$$

For the MIMO feedback system the size of the smallest additive uncertainty destabilizing the feedback system can be derived as follows:

$$\bar{\sigma}[\Delta_a(j\omega)] = \frac{1}{\bar{\sigma}[K_s K_c S(j\omega)]} \quad (5.11)$$

Condition of robust stability defined by eq (5.7) was analyzed and the closed loop system given in Fig 3. was tested for this inequality. Results of the computer simulation can be seen in Fig 9.

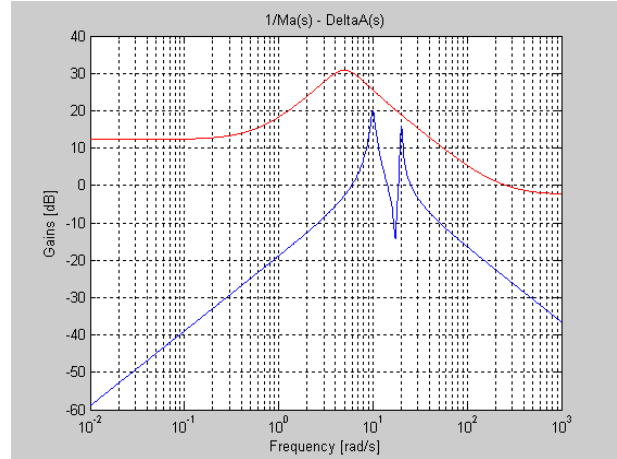


Fig 9. The Inverse Sensitivity Transfer Function and the Additive Uncertainty Gain
 $1/Ma(s)$ $\Delta A(s)$

From Fig 9. it is evident that magnitude of the transfer function seen by the additive uncertainty of $M_a(s)$ larger than the additive uncertainty gain of $|\Delta_a(s)|$: i.e. closed loop control system of the longitudinal stability augmentation system working with simple static controller of K_c can be said robustly stable. For uncertainty given by eqs (2.13)-(2.14) additive stability margin is, $ASM = 4,4874$.

6. SUMMARY AND CONCLUSIONS

The paper dealt with basic equations of the aircraft elastic motion. The transfer function of the elastic aircraft was derived. The high frequency dynamics generated by elevator deflection has been involved as additive uncertainty. The closed loop control system of the aircraft longitudinal stability augmentation system was analyzed for the 1st and for the 2nd overtones of the fuselage elastic motion. The transient behavior, Bode diagrams and the dynamic performances were derived and analyzed. The robust stability was derived using small gain theorem for additive uncertainty. It was stated that for the given

uncertainty the closed loop system is robustly stable even when it is equipped with static controller.

REFERENCES

1. Dr. habil. Szabolcsi, R. *Robust Analysis of the Automatic Control Systems*, Proceedings of the International Conference on Military Technologies ICMT'07, ISBN 978-80-7231-238-2, pp (447-454), University of Defense, Faculty of Military Technologies, Brno, Czech Republic (2007).
2. Dr. habil. Szabolcsi, R. *Robust Analysis of the Stability Augmentation Systems*, Proceedings of the International Conference on Military Technologies ICMT'07, ISBN 978-80-7231-238-2, pp(455-463), University of Defense, Faculty of Military Technologies, Brno, Czech Republic (2007).
- [3] Bisplinghoff, R. L. – Ashley, H.: – Halfman, R. L. *Aeroelasticity*, Addison–Wesley Publishing Company, Inc., Cambridge, Mass. (1955).
- [4] Bisplinghoff, R. L. – Ashley, H.: *Principles of Aeroelasticity*, John Wiley and Sons, Inc., New York–London (1962).
- [5] Асланян, А. Э.: *Системы автоматического управления полётом летательных аппаратов*, Часть I, Киевское Высшее Военное Авиационное Инженерное Училище, Киев (1984).
- [6] Красовский, А. А. – Вавилов, Ю. А. – Сучков, А. И.: *Системы автоматического управления летательных аппаратов*, Издание ВВИА им. проф. Н. Е. Жуковского, Москва (1986).
- [7] McLean, D.: *Automatic Flight Control Systems*, Prentice-Hall International, New York-London-Toronto-Sydney-Tokyo-Singapore (1990).
- [8] MIL–F–9490D *Notice 1, Flight Control Systems – Design, Installation, and Test of Piloted Aircraft, General Specification* (1992).
- [9] Shahian, B. – Hassul, M.: *Control System Design using MATLAB®*, Prentice-Hall, Englewood Cliffs, New Jersey (1993).
- [10] MIL–C–18244A, *Amendment 1, Control and Stabilization System: Automatic, Piloted Aircraft, General Specification* (1993).
- [11] Dowell, E. H.: *A Modern Course in Aeroelasticity*, Kluwer Academic Publishers, Dordrecht–Boston–London (1995).
- [12] Szabolcsi, R.: *Design of the Pitch Attitude Control System for the Aeroelastic Fighter Aircraft*, Bulletins for Applied Mathematics, BAMB-1240/96, LXXX., pp(29-40), 10-13 October, 1996, Göd, Hungary.
- [13] MIL–F–8785C, *Notice 2, Flying Qualities of Piloted Airplanes* (1996).
- [14] Szabolcsi, R. – Gáspár, P.: *Flight Control System Synthesis for the Aeroelastic Jet Fighter Aircraft*, Preprints of the IFAC Symposium on Robust Control Design, ROCOND '97, p(453-458) (1997).
- [15] Nelson, R. C.: *Flight Stability and Control*, McGraw-Hill Companies, Inc., 1998.
- [16] Control System Toolbox 5.1 for Use With MATLAB® (Release 12.1), User's Guide, The MathWorks, Inc. (2001).
- [17] Szabolcsi, R. – Szegedi, P.: *Design of the Chebishev BR Filter for the Elastic Aircraft Longitudinal Stability Augmentation System*, Proceedings of the “1st International Symposium on Future Aviation Technologies FAT 2002”, Vol. 1., pp (43–52), April 12–14, 2002, Szolnok, Hungary.
- [18] MATLAB® 6.5 — The Language of Technical Computing, User's Guide, The MathWorks, Inc. (2002).
- [19] Dr. Palik, M. Pilóta nélküli repülőgépek üzemeltetésének légiközlekedés-biztonsági szempontjai. “XVII. Magyar Repüléstudományi Napok” tudományos konferencia kiadványa, pp(1-16), ISBN 978-963-3130-32-2, Budapest, Hungary.
- [20] Dr. Palik, M. – Vas, T. UAV Operations in Aerodrome Safety and ACS Procedures. Proceedings of the International Conference “Defense Resources Management in the 21st Century”, ISSN 2248-2385, pp(75-89), Brasov, Romania.